International Journal of Thermal Sciences 49 (2010) 762–768

Contents lists available at ScienceDirect

International Journal of Thermal Sciences

journal homepage: www.elsevier.com/locate/ijts

Real-time solution of heat conduction in a finite slab for inverse analysis

Z.C. Feng*, J.K. Chen, Yuwen Zhang

Department of Mechanical and Aerospace Engineering, University of Missouri, Columbia, MO 65211, USA

ARTICLE INFO

Article history:
Received 6 July 2009
Received in revised form
30 October 2009
Accepted 1 November 2009
Available online 22 November 2009

Keywords:
Inverse problem
Transfer function
Sensor compensation
Temperature measurement

ABSTRACT

Laplace transform is used to solve the problem of heat conduction over a finite slab. The transfer functions relating the temperature and heat flux on the front and back surfaces of the finite slab are developed. Although there are many competing methods for constructing the inverse Laplace transform, we use polynomial approximation of the transfer function. Therefore, transient solutions for given boundary conditions are easily obtained using SIMULINK. This process is much simpler than other numerical solution methods for the heat equation. Most importantly, our method of solution allows us to obtain, in real-time, the front surface temperature and heat flux based on the thermodynamic measurements on the back surface. We also demonstrate the feasibility of reconstructing the front surface temperature when sensor noise is incorporated to the back surface measurements.

1. Introduction

In measurements of surfaces with high temperatures, there are situations when direct measurements of temperature and heat flux are not feasible. A surface heated by high intensity laser is an example. Conventional sensors can hardly withstand the intense heat. Measurements from noncontact sensors are affected by the out-gassing from the heated surface in the case of a composite target. In the case of a metal target, the noncontact sensor measurements often have large uncertainty since radiation from a metal target deviates significantly from that of a black body.

One strategy to overcome the difficulty is to instrument sensors on the back surface of the heated target. The sensors can function since they are not directly exposed to the high energy input. The objective then is to infer the front surface temperature and heat flux from the back surface measurements. Under these circumstances, the front surface temperature can be determined indirectly by solving an inverse heat conduction problem [1–3] based on the transient temperature or/and heat flux measured at the back surface.

In the mathematical formulation of the inverse problem, either temperature or heat flux can be measured at the back surface. Most previous researchers prefer temperature measurements because temperature can be measured with fewer uncertainties compared to heat flux measurements [4–7]. However, recent studies have showed that using measured heat flux as additional information in the formulation of an IHCP can increase the stability of the solution and is less prone to the inherent instability of the ill-posed problem of inverse heat conduction [8,9].

In this paper, we propose an alternative approach to solving the inverse heat conduction problem. Laplace transform is used to obtain the relationship between temperature and heat flux of the two surfaces. These relationships are given as transfer functions. By introducing polynomial approximations, we can implement numerical solutions using SIMULINK. The numerical solutions on the back surface are used to simulate sensor measurements. With noise added to the sensor measurement, we investigate whether the front surface temperature and heat flux can be reconstructed.

In the following section, we specify the heat conduction problem and simplify the resulting equation through non-dimensionalization. Starting in Section 3, we use Laplace transform to develop the transfer functions relating the temperature and heat flux between the front and back surfaces when the back surface temperature is held fixed. Approximations of the transfer functions are subsequently obtained through matching poles and zeros. The approximate transfer functions are implemented in SIMULINK. Solutions are obtained for prescribed front surface heat flux input. In Section 4, we add noise to the back surface measurement. We again use the transfer functions to reconstruct the front surface heat flux and temperature. In Section 5, we study the transfer function in the frequency domain to illustrate the reason behind the difficulty in reconstructing the front surface quantities in the presence of sensor noise. In Section 6, we obtain the transfer function for another important boundary condition: the case when

* Corresponding author. Tel.: +1 573 884 4624; fax: +1 573 884 5090.
E-mail addresses: fengf@missouri.edu (Z.C. Feng), chenjnk@missouri.edu (J.K. Chen), zhangyu@missouri.edu (Y. Zhang).

1290-0729/$ – see front matter © 2009 Elsevier Masson SAS. All rights reserved.
doi:10.1016/j.ijthermalsci.2009.11.002

Nomenclature

c_{ps}	mass specific heat of the slab, J/(kg K)
G	transfer function for the fixed back surface temperature
H	transfer function for the convective back surface boundary condition
h	dimensionless convective heat transfer coefficient
k_s	thermal conductivity, W/(m K)
L	thickness of 1-D slab, m
p	pole of a transfer function
q	heat flux, W/m^2
Q	Laplace transform of the heat flux
t	time, s
t_c	characteristic time, s
T_s	temperature of the slab above the ambient temperature, K
U	Laplace transform of temperature
x	spatial coordinate variable, m
z	zero of a transfer function

Greek symbols

ρ_s	density of the slab, kg/m^3
τ	dimensionless time
ω	dimensionless frequency
ξ	dimensionless length variable

Subscripts

b	back surface quantity
f	front surface quantity

the back surface has a convective boundary condition. Conclusions of the present work are given in Section 7.

2. The mathematical model

Consider heat conduction over a finite slab, Fig. 1. Assume that the solid has a constant thermal conductivity. The governing equation is given by the following:

$$\rho_s c_{ps} \frac{\partial T_s}{\partial t} = k_s \frac{\partial^2 T_s}{\partial x^2} \tag{1}$$

where ρ_s, k_s and c_{ps} are the density, thermal conductivity and specific heat of the solid.

Since the one dimensional model here represents an approximation of a sheet-like three-dimensional body when the temperature gradient along the sheet is ignored, it is thus more intuitive to regard $x = 0$ and $x = L$ as the "front" and the "back" surfaces of the sheet-like solid. Our main interest here is to use the measurements from the back surface to determine the temperature and the heat flux on the front surface.

To simplify the problem further, we choose the sheet thickness L as the characteristic length and the constant

$$t_c = \frac{\rho_s c_{ps} L^2}{k_s} \tag{2}$$

as the characteristic time. Thus we simplify the governing equation to

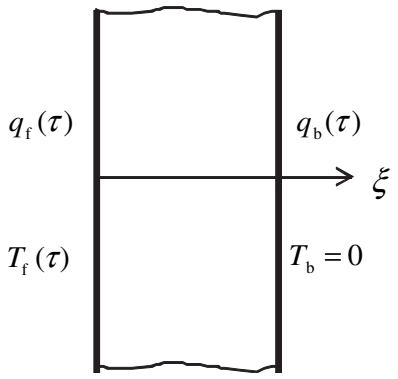

Fig. 1. Heat conduction over a finite slab. The back surface is assumed to be in contact with a heat sink.

$$\frac{\partial T_s}{\partial \tau} = \frac{\partial^2 T_s}{\partial \xi^2} \quad \text{for } 0 < \xi < 1 \tag{3}$$

where $\tau = t/t_c$ and $\xi = x/L$ now represent the dimensionless time and dimensionless position across the thickness.

To obtain the relationships between the measurements on the front and the back surface, we consider two specific cases. The first case corresponds to boundary conditions specified on the back surface. Specifically, we assume that the temperature on the back surface is maintained at constant while the heat flux is obtained from a sensor. A constant back surface temperature can be maintained through a reservoir containing ice-water mixture. An alternative approach is to set up evaporation on the back surface, in which case the back surface temperature can be adjusted to any value by adjusting the vapor pressure on the back. In either case, we have on the back surface, i.e. at $\xi = 1$,

$$T_s = 0 \tag{4a}$$

$$-\frac{\partial T_s}{\partial \xi} = q_b \tag{4b}$$

where q_b is normalized heat flux (K) at the back surface and the actual back surface heat flux is $q_b k_s/L$ (W/m^2).

The second case has convective boundary condition on the back surface. Namely, at $\xi = 1$,

$$-\frac{\partial T_s}{\partial \xi} = hT_b \tag{5}$$

where h is a constant that represents the dimensionless convective heat transfer coefficient. The convective heat transfer coefficient for the physical problem is hk_s/L. For this boundary condition, the back surface heat flux and temperature are proportional to each other. When h is large, this case should approach the first case above.

3. Transfer functions and transient solutions

Applying the Laplace transform [10,11] to equation (3), we obtain the following equation

$$sU(\xi) = \frac{d^2 U(\xi)}{d\xi^2}. \tag{6}$$

where $U(\xi)$ is the Laplace transform of $T_s(\xi, \tau)$. The solution of the resulting equation is written as

$$U = c_1 e^{\sqrt{s}\xi} + c_2 e^{-\sqrt{s}\xi} \tag{7}$$

Applying the boundary condition (4a), we have

$$U = c_1\left[e^{\sqrt{s}\xi} - e^{\sqrt{s}(2-\xi)}\right] \tag{8}$$

If we let Q_f and Q_b denote the Laplace transform of the heat flux at the front and the back surfaces respectively, we have

$$\frac{Q_b}{Q_f} = \frac{\frac{dU(\xi=1)}{d\xi}}{\frac{dU(\xi=0)}{d\xi}} = G_1(s) \tag{9}$$

where

$$G_1(s) = \frac{1}{\cosh\sqrt{s}}. \tag{10}$$

Similarly, let U_f denote the Laplace transform of the front surface temperature. We obtain

$$\frac{U_f}{Q_f} = \frac{U(\xi = 0)}{-\frac{dU(\xi=0)}{d\xi}} = G_1(s)G_2(s), \tag{11}$$

where

$$G_2(s) = \frac{\sinh\sqrt{s}}{\sqrt{s}}. \tag{12}$$

For the heat conduction problem defined above, the back surface temperature is set to zero. If one more boundary condition is prescribed, solutions are obtained from the transfer functions. Specifically, if the front surface heat flux, $q(0,\tau)$, is given, its Laplace transform, i.e. Q_f, is obtained. Consequently, the back surface heat flux is given by the inverse Laplace transform of the following:

$$Q_b = G_1(s)Q_f \tag{13}$$

and the front surface temperature:

$$U_f = G_1(s)G_2(s)Q_f. \tag{14}$$

To obtain the temperature and heat flux in the time domain, inverse Laplace transform must be found. The analytical form of the inverse Laplace transform is possible only for a few very special cases [10,11]. Motivation to our work is to obtain one quantity from another measured quantity. For example, we are interested to obtain the front surface temperature from the back surface heat flux. Therefore, a purely numerical solution is satisfactory. In the literature, numerical solutions are obtained through numerical inverse of the transfer function. Because of the convenience of Laplace transform method for various physical problems, there are well over 100 different algorithms available for calculating the inverse Laplace transform [12–15].

In dynamical systems literature, time domain solutions are obtained from the transfer functions without the explicit inverse of the Laplace transform. When the transfer functions are expressed as polynomials, the underlying dynamical systems are conveniently expressed as ordinary differential equations; time domain solutions are obtained directly through numerical solutions of the ordinary differential equations [16]. However, the transfer functions here are not in polynomial forms since they are derived from a continuous system governed by a partial differential equation. Approximation to the transfer function using polynomials, which preserve the poles and zeros, has been used in dynamical systems to cope with this difficulty [17].

By solving the nonlinear algebraic equation corresponding to zero denominator for function $G_1(s)$, we obtain the poles of the transfer function $G_1(s)$ at

$$s = p_k = -\left[\frac{(2k-1)\pi}{2}\right]^2, k = 1,2,3,\ldots \tag{15}$$

Setting the numerator of function $G_2(s)$ to zero and solving the resulting nonlinear algebraic equation, we obtain the zeros of the transfer function $G_2(s)$ at

$$s = z_k = -(k\pi)^2, k = 1,2,3,\ldots \tag{16}$$

Therefore, we have the following approximations for the transfer functions:

$$G_1(s) \approx \frac{p_1p_2p_3p_4p_5p_6}{(s-p_1)(s-p_2)(s-p_3)(s-p_4)(s-p_5)(s-p_6)} \tag{17}$$

$$G_2(s) \approx \frac{(s-z_1)(s-z_2)(s-z_3)(s-z_4)}{z_1z_2z_3z_4} \tag{18}$$

where up to 6th order terms are kept for $G_1(s)$ and up to 4th order terms are kept for $G_2(s)$. It is easy to keep more terms at the cost of computation time. However, since the product of these two functions is required in (14), the order of the polynomial in the denominator must be higher than the order of the numerator (Fig. 2).

To understand the limitation of the approximate transfer functions above, we have compared the "gain" and the "phase angle" of the approximate transfer functions. For $\omega \le 20$, the graphs of gains of each transfer function and its approximation exactly overlap. However, the phase angles of the approximate transfer functions have more noticeable deviations. These discrepancies are shown in Fig. 3. For both transfer functions, starting from zero at $\omega = 0$, the phase angle differences increase with the frequency ω. Therefore, the approximation is acceptable if ω is small.

As another way to illustrate the validity of the polynomial approximation to the transfer functions, we examine a special case for which solution of the heat equation can be obtained analytically. Consider the case when the front surface heat flux is a constant. The Laplace transform of the heat flux $Q_f = 1$. Therefore, the Laplace transform of the front surface temperature is the product of the two transfer functions $G_1(s)$ and $G_2(s)$ respectively. When polynomial approximations in (17) and (18) are used as the approximations to the transfer function, the inverse Laplace transform is easily obtained. Although the resulting algebraic expression is very cumbersome, the front surface temperature is plotted as a function of time. In Fig. 4, we show the front surface temperature obtained this way superimposed on the analytical solution given below:

$$T_s(\tau,\xi) = (1-\xi)q_0 + \sum_{n=1}^{\infty} c_n e^{-\lambda_n^2\tau}\cos\lambda_n\xi \tag{19}$$

where

$$\lambda_n = -\frac{(2n-1)}{2}\pi, \tag{20}$$

$$c_n = -\frac{8q_0}{(2n-1)^2\pi^2}. \tag{21}$$

Note that the two curves are nearly indistinguishable.

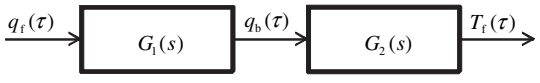

Fig. 2. Simulation block diagram.

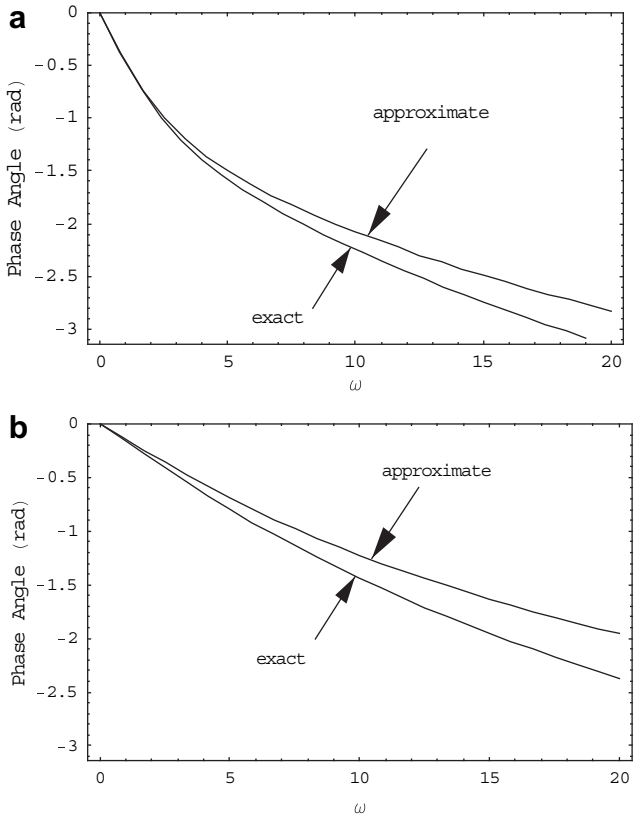

Fig. 3. Errors of the approximate transfer functions: (a) phase angle of the transfer functions $G_1(j\omega)$ and its approximation; (b) phase angle of the transfer functions $1/G_2(j\omega)$ and its approximation.

To illustrate the simplicity of the solution for time dependent inputs, we set the front surface heat flux to

$$q_f(\tau) = 40 + 4\sin 3\tau. \tag{22}$$

The back surface heat flux and the front surface temperature are easily obtained using SIMULINK. They are shown in Fig. 5. Therefore, by implementing the approximate transfer functions in SIMULINK, we can easily obtain transient solutions to the heat conduction problem.

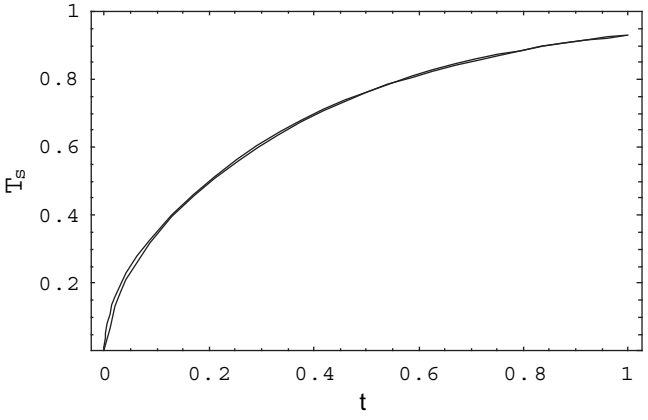

Fig. 4. Front surface temperature of a slab subjected to constant heat flux on the front surface. The two indistinguishable curves correspond to the solution from the approximate transfer function and the analytical solution of the original heat equation.

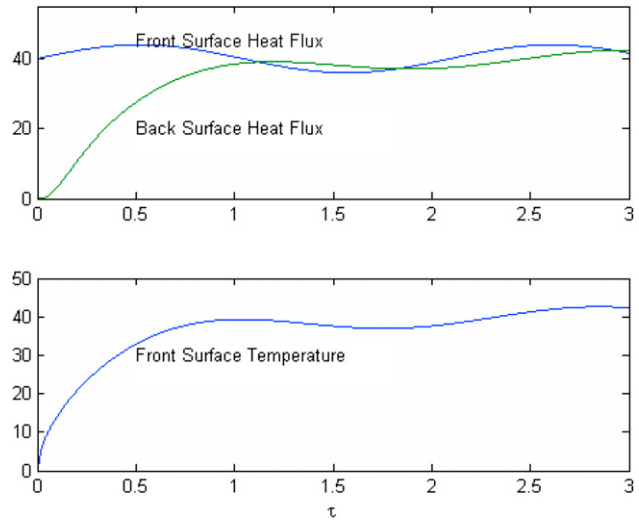

Fig. 5. Results obtained using SIMULINK when the front surface heat flux is a sinusoid with a bias.

4. Calculation of the front surface temperature and heat flux from back surface measurement

The transfer functions we have obtained allow us to reconstruct the front surface temperature and heat flux from the back surface measurement. Numerical solutions obtained in the above section can be used as measured values from the back surface. In order to show that this method is robust to sensor uncertainties, we add noise to the back surface heat flux obtained from simulation results given in the above section. The block diagram is shown in Fig. 6.

Specifically, from the heat flux measurement, we can obtain the front surface heat flux and temperature since:

$$Q_f = \frac{1}{G_1(s)} Q_b \tag{23}$$

and

$$U_f = G_2(s) Q_b. \tag{24}$$

The noise we have introduced into the back surface heat flux is generated using the "band-limited white noise" generator of SIMULINK with sampling time of 0.001. The strength of the noise is quantified by the "noise power". Since this noise is discontinuous, it is filtered by a fourth order Butterworth low-pass filter with the dimensionless cut-off frequency set at 40. The resulting signal is added to the heat flux solution given in Fig. 5. The back surface heat flux with noise is shown in the top panel of Fig. 7. Corresponding to noise power of 0.01, the reconstructed front surface temperature and heat flux are shown in the bottom two panels of Fig. 7. Since the transfer functions contain time derivatives, noise becomes much

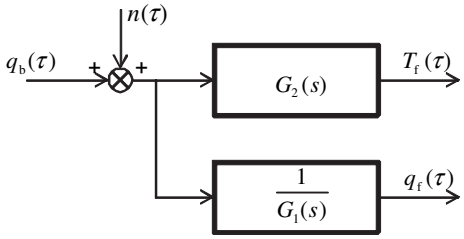

Fig. 6. Block diagram for the reconstruction of the front surface temperature and heat flux from the back surface heat flux measurement in the presence of sensor noise.

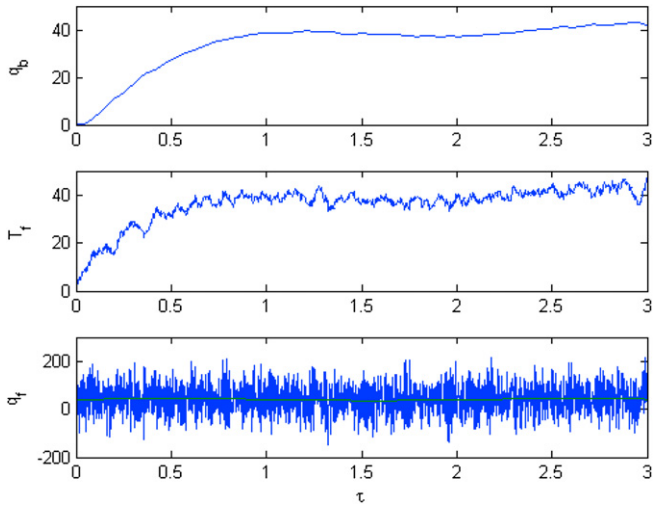

Fig. 7. Front surface temperature and heat flux reconstructed from the back surface heat flux measurement when a noise with "noise power" 0.01 is added to back surface heat flux.

more significant in the reconstructed temperature. However, the reconstructed temperature agrees with that given in Fig. 5 if appropriate average is applied. The same is not true for the reconstructed front surface heat flux. Noise overwhelms the underlying trend. Front surface heat flux can be recovered for much smaller "noise power". When the noise power is 0.00001, the recovered quantities are shown in Fig. 8. From these tests, we see that heat flux reconstruction is more difficult that the temperature.

5. The frequency response function

In the above section, we have observed that front surface temperature reconstruction can tolerate more sensor noise. To rule out the possibility that such an observation is an artifact of the approximation introduced for the transfer functions, we study the transfer functions in the frequency domain. This study does not require that the transfer functions be polynomials. Therefore, no approximation for the transfer functions is required.

Consider the transmission from the front surface temperature to the back surface heat flux. Let $s = j\omega$ where $j = \sqrt{-1}$ we have the relationship from (24)

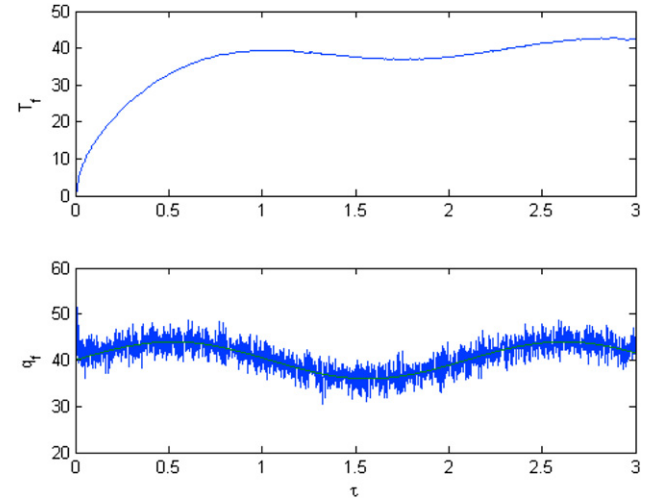

Fig. 8. Front surface temperature and heat flux reconstructed from the back surface heat flux measurement when a noise with "noise power" 0.00001 is added to the results in Fig. 5.

$$\frac{Q_b(j\omega)}{U_f(j\omega)} = \frac{1}{G_2(j\omega)} \tag{25}$$

We use the exact transfer function to obtain the frequency response function as shown in Fig. 9. We observe that the heat conduction from the front surface to the back surface is "low-pass" in nature. High frequency fluctuations are averaged out. Similarly, we can also obtain the frequency response function representing the transmission from the front surface heat flux to the back surface heat flux as follows.

$$\frac{Q_b(j\omega)}{Q_f(j\omega)} = G_1(j\omega) \tag{26}$$

The gain and the phase angle as functions of frequency are shown in Fig. 10. We note that for this latter case, the gain decays much faster as frequency increases. In other words, fluctuations in the front surface heat flux get averaged out as the heat conducts through the slab. It thus can be expected that reconstructing the front surface heat flux from the back surface heat flux measurement does not allow much uncertainties in the sensor measurement.

For conventional sensors such as load cells and accelerometers, the frequency response function is used to quantify the sensor dynamic response. Since the signal to be measured may contain multiple frequencies, the sensor measurement is considered sufficiently accurate within a given frequency range when the gain remains nearly constant and the phase remains zero. The requirement on the phase angle can be relaxed under one circumstance. If the phase angle of the transfer function is proportional to the frequency, the sensor is known to introduce a "dead" time delay [18]; a "dead" time delay introduced by the sensor does not distort the

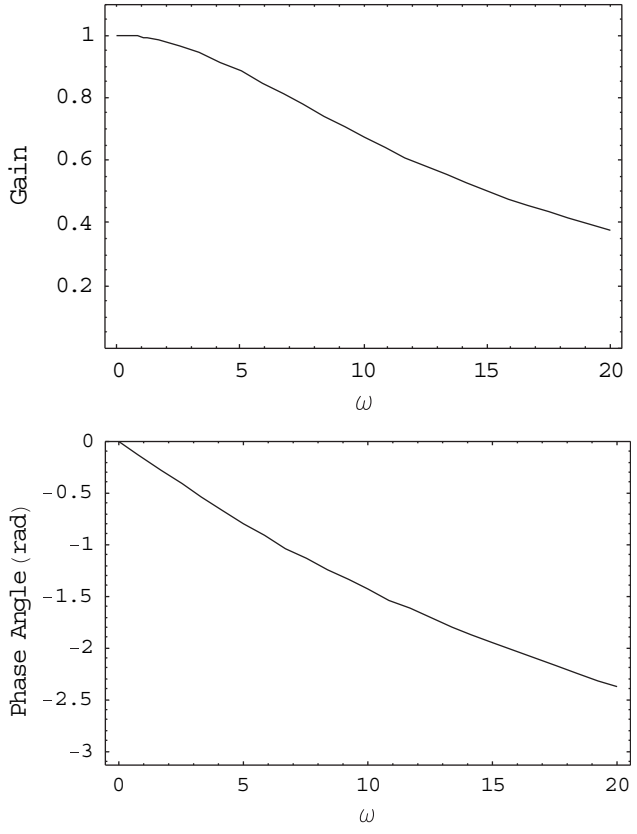

Fig. 9. Frequency response function $Q_b(j\omega)/U_f(j\omega)$. The function represents the transfer function from the front surface temperature to the back surface heat flux. $Q_b(j\omega)/Q_f(j\omega)$.

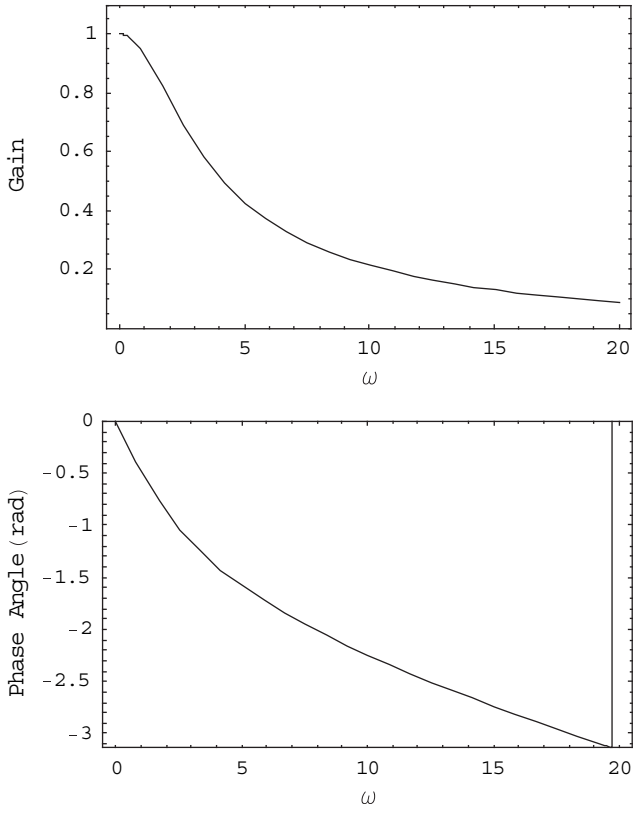

Fig. 10. Frequency response function $Q_b(j\omega)/Q_f(j\omega)$. The function represents the transfer function from the front surface heat flux to the back surface heat flux.

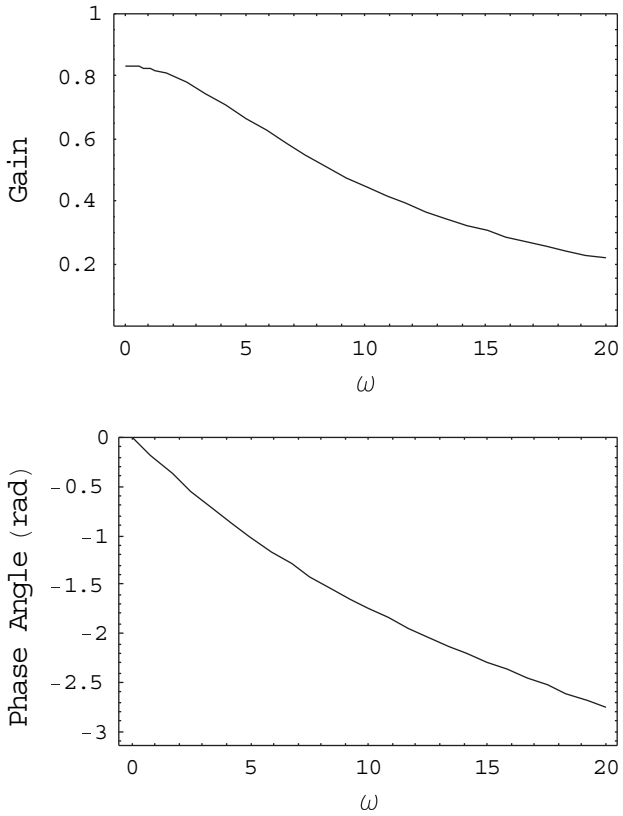

Fig. 11. Frequency response function $Q_b(j\omega)/U_f(j\omega)$. The function represents the transfer function from the front surface temperature to the back surface heat flux. $h = 5$.

wave form. Therefore, the requirement on the sensor frequency response can be relaxed to that the gain remains nearly constant and the phase angle is proportional to the frequency. Examining Fig. 9, we can roughly say that for $0 < \omega < 3$, the back surface heat flux measurement can directly be used as the estimation for the front surface temperature. In Fig. 10, the gain changes more drastically with the frequency. Perhaps we may regard the gain to be nearly constant and the phase angle to be nearly linear for $0 < \omega < 1$. Therefore, the back surface heat flux can be directly used as the estimation of the front heat flux only for a much lower frequency.

The approach in Section 4 is a method for compensating the deficiency of the direct measurement results. The compensation is accomplished based on the known mathematical model of the heat conduction problem. The dynamic range is extended since the transfer functions for reconstructing front surface temperature and heat flux represent time derivatives. In SIMULINK implementation, the front surface measurements are obtained based on the back surface measurement and its time derivatives. The order of polynomial approximations determines the highest order derivatives that are included. Therefore, the reconstructed front surface quantities are linear combinations of the back surface measurement and its derivatives. The coefficients of the polynomials determine the "weights" (proportions) of derivative terms.

The gain in Fig. 10 shows a more steep decrease with frequency than that in Fig. 9. Consequently, the compensation required to extend the dynamic range will thus involve more "weights" in the time derivatives. Numerical derivatives are sensitive to noise. Reconstructing the front surface heat flux will require more weights in derivative terms. It is thus not surprising that reconstructing the front surface heat flux is not possible unless the sensor noise is small.

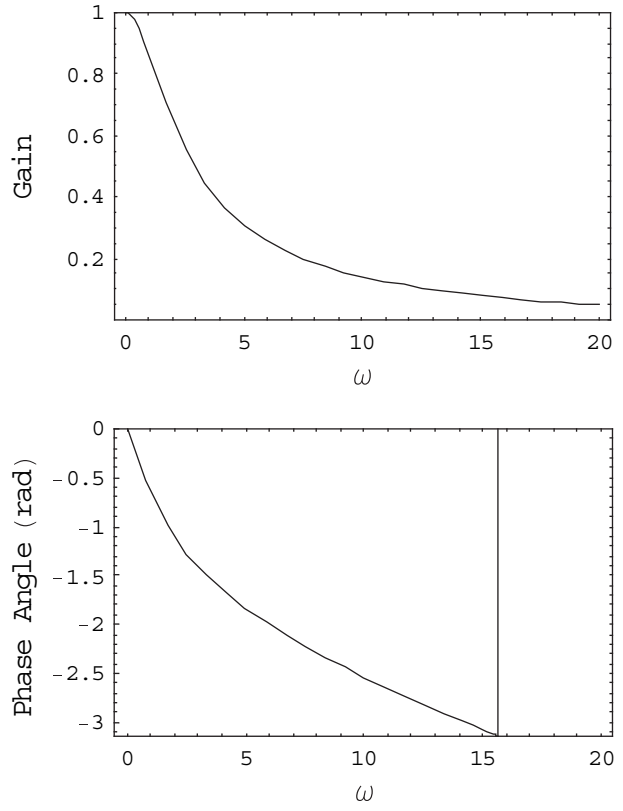

Fig. 12. Frequency response function $Q_b(j\omega)/Q_f(j\omega)$. The function represents the transfer function from the "net" front surface heat flux to the back surface heat flux. $h = 5$.

6. Transfer function with convective boundary condition on the back surface

The second case corresponds to "mixed" boundary conditions that neither the heat flux nor the temperature is prescribed. Specifically, this case includes convection boundary conditions:

$$-\frac{\partial T_s}{\partial \xi} = q_f \quad \text{at } \xi = 0 \tag{27}$$

$$-\frac{\partial T_s}{\partial \xi} = hT_b \quad \text{at } \xi = 1 \tag{28}$$

where $q_f k_s/L$ is the heat flux imposed on the front surface; hk_s/L is the convection heat transfer coefficient on the back surface. Note that on the back surface, the heat flux and the temperature are proportional to each other.

Substituting (7) into (28), we obtain the following:

$$U = c_1\left[e^{\sqrt{s}\xi} - \frac{h+\sqrt{s}}{h-\sqrt{s}}\,e^{\sqrt{s}(2-\xi)}\right] \tag{29}$$

The following transfer functions are obtained:

$$\frac{Q_b}{Q_f} = H_1(s) \tag{30}$$

$$\frac{U_f}{Q_f} = H_1(s)H_2(s) \tag{31}$$

where

$$H_1(s) = \frac{1}{\cos h\sqrt{s} + \frac{\sqrt{s}}{h}\sin h\sqrt{s}} \tag{32}$$

and

$$H_2(s) = \frac{\sin h\sqrt{s}}{\sqrt{s}} + \frac{1}{h}\cos h\sqrt{s} \tag{33}$$

For the convective boundary condition, the back surface temperature is no longer a constant. Heat transfer rate through the slab is lower than the previous case. As shown in Figs. 11 and 12, the gains of the transfer functions decrease as the frequency increases. Therefore, the front surface temperature or heat flux fluctuations are in effect "averaged out" through the slab. Reconstructing the front surface quantities is limited to low frequencies in the presence of sensor noise. Similar to the previous case, the sensor noise must be lower still if we wish to reconstruct the front surface heat flux from the back surface heat flux.

Similar to the previous case, the transfer functions can be approximated by polynomials which have the same zeros and poles; the poles and zeros of the transfer functions can be solved numerically for given values of h. The approximate transfer functions can thus be used to reconstruct the front surface temperature and heat flux based on the back surface heat flux measurement. We note that for this boundary condition, the back surface temperature and heat flux are proportional to each other.

7. Conclusions and discussions

In this paper, we obtained solutions to the heat conduction problem in terms of transfer functions. These transfer functions, upon approximation by polynomials, can be used to obtain numerical solutions for given boundary conditions using tools in system dynamics such as SIMULINK. With these tools, it is very convenient to reconstruct the front surface temperature and heat flux from the back surface measurement. The most practical aspect of our method is that the front surface temperature can be obtained in real-time. Consequently, the amount of data processing is greatly reduced.

Our method is an alternative to methods for the "inverse heat conduction problem" [1–3]. The method proposed here is much simpler. Our method is limited to linear problems. However, Laplace transform has been applied to non-homogeneous materials [19,20] by many investigators; it remains to be seen whether approximations of transfer functions can provide sufficiently accurate solutions to these complicated problems.

Finally, our method represents an approach to solving the heat equation through integral transforms. Such an approach has been formulated in a systematic fashion in methods known as "thermal quadrupoles" [21]. The polynomial approximation to the resulting transfer functions can be combined with the thermal quadrupoles to result in a complete "system dynamics" approach to the heat conduction problem.

Acknowledgement

We thank the reviewers for their very helpful suggestions and for bringing to our attention works on thermal quadrupoles.

References

[1] J.V. Beck, B. Blackwell, C.R. St-Clair, Inverse Heat Conduction: Ill Posed Problems. Wiley, New York, 1985.
[2] O.M. Alifanov, Inverse Heat Transfer Problems. Springer-Verlag, Berlin/Heidelberg, 1994.
[3] M.N. Özisik, H.R.B. Orlande, Inverse Heat Transfer: Fundamentals and Applications. Taylor & Francis, New York, 2000.
[4] T.E. Diller, Advances in heat flux measurements. Advances in Heat Transfer 23 (1993) 279–368.
[5] P.R.N. Childs, J.R. Greenwood, C.A. Long, Heat flux measurement techniques. Proceedings of the Institute of Mechanical Engineers. Part C: Journal of Mechanical Engineering Science 213 (C7) (1999) 655–677.
[6] A. Tong, Improving the accuracy of temperature measurements. Sensor Review 21 (3) (2001) 193–198.
[7] P.R.N. Childs, Advances in temperature measurement. Advances in Heat Transfer 36 (2002) 111–181.
[8] A. Saidi, J. Kim, Heat flux sensor with minimal impact on boundary conditions. Experimental Thermal and Fluid Science 28 (2004) 903–908.
[9] T. Loulou, E.P. Scott, An inverse heat conduction problem with heat flux measurements. International Journal for Numerical Methods in Engineering 67 (2006) 1587–1616.
[10] M.N. Ozisik, Heat Conduction, second ed.. Wiley-Interscience, New York, 1993.
[11] G.E. Myers, Analytical Methods in Conduction Heat Transfer, second ed. AMCHT Publications, Madison, WI, 1998.
[12] J. Abate, P.P. Valko, Multi-precision Laplace transform inversion. International Journal for Numerical Methods in Engineering 60 (2004) 979–993.
[13] B. Davies, B. Martin, Numerical inversion of the Laplace transform: a survey and comparison of methods. Journal of Computational Physics 33 (1979) 1–32.
[14] G.V. Narayanan, D.E. Beskos, Numerical operational methods for time-dependent linear problems. International Journal for Numerical Methods in Engineering 18 (1982) 1829–1854.
[15] D.G. Duffy, On the numerical inversion of Laplace yransform: comparison of three new methods on characteristic problems from applications. ACM Transactions on Mathematical Software 19 (1993) 333–359.
[16] K. Ogata, System Dynamics, third ed. Prentice Hall, New Jersey, 1998.
[17] S.D. Eppinger, W.P. Seering, Modeling robot flexibility for endpoint force control, in: Proceedings of 1988 IEEE International Conference on Robotics and Automation, April 24–29, 1988, Philadelphia, PA, USA, pp. 165–170.
[18] E.O. Doebelin, Measurement Systems: Application and Design, fifth ed. McGraw Hill, New York, 2004.
[19] A. Sutradhar, G.H. Paulino, L.J. Gray, Transient heat conduction in homogeneous and non-homogeneous materials by the Laplace transform Galerkin boundary element method. Engineering Analysis with Boundary Elements 26 (2002) 119–132.
[20] G.E. Cossali, Dynamic response of a non-homogeneous 1D slab under periodic thermal excitation. International Journal of Heat and Mass Transfer 50 (2007) 3943–3948.
[21] D. Maillet, S. Andre, J.C. Batsale, A. Degiovanni, C. Moyne, Thermal Quadrupoles: Solving the Heat Equation through Integral Transforms. John Wiley & Sons, New York, 2000.